

Supplemental Figure Legends

Fig. S1. Electrical coupling of Rin cell pairs following transfection with either Cx50 or Cx50(S395A) mutant. (A) The coupling frequency (number of coupled cell pairs relative to total number of cell pairs explored) for each group was similar (wt = 0.58; wt+8Br = 0.58; S395A = 0.56; S395A+8Br = 0.44). (B) Level of electrical coupling (g_j) in cell pairs where both cells were reliably recorded (white circles represent mean \pm s.e.m.). No difference ($p > 0.1$) was found for Cx50 between untreated (13.8 ± 2.9 nS; $n = 39$) and 8-Br-cAMP treated (18.2 ± 6.4 nS; $n = 11$); in contrast, for Cx50(S395A) a significant ($p < 0.01$) reduction in coupling was induced by PKA activation: untreated pairs (19.0 ± 4.4 , $n = 19$) and treated (3.6 ± 1.0 , $n = 4$). To account for range variability, the data are also displayed in box plots, where the internal line is the median, the whisker and box side closer to zero are the 10th and 25th percentiles, the box side and whisker farther from zero are the 75th and 90th percentiles, and the black circles denote the outliers. (C) Absolute values of electrical coupling as a function of days post-transfection. Empty circles: untreated Cx50; gray triangles: untreated Cx50(S395A) mutant.

Fig. S2. Channel transitions between open states as well as between the closed and open states were observed in voltage-clamp channel recordings. Primary records and associated all point histograms of Cx50 illustrating residual states under control conditions (A and B) and large, ≥ 200 pS, transitions under control (C) and 8-Br-cAMP treatment conditions (D). Black and grey arrows respectively mark the start and end of voltage pulses, except for trace in D, where the end of a longer pulse is not displayed. Calibration for all traces: $y = 10$ pA; $x = 2$ s, transjunctional voltage was ± 40 mV. Dashed lines mark zero transjunctional current level. All point histograms at the right of every trace are labeled with cumulative conductance values relative to baseline (0 pS). Conductance values on the left indicate the conductance differences between dotted current level lines, whereas values near events indicate the conductances of those transitions.

Fig. S3. The untreated Cx50(S395A) mutant junctions display altered channel behavior. The plot of differences between the events histograms of untreated Cx50(S395A) and untreated Cx50 (A) shows that the mutation *per se* is sufficient to decrease the frequency of transitions between the residual and ~ 200 pS open state, and increase the frequency of transitions between the closed and ~ 200 pS open state. This plot suggests that untreated Cx50(S395A) mutant channels transit more frequently from fully closed to fully open, and possibly to a higher conductive state. Consequently, the differences between the untreated Cx50(S395A) and the 8-Br-cAMP treated Cx50 (B) are minimal, suggesting that phosphorylation at Ser395 is not required for the PKA-induced alteration of channel behavior.

Fig. S4. PKA activation minimally affects the open time of Cx50 (A) or Cx50(S395A) mutant (B) channels. Absolute time between the opening and subsequent closing transitions of events, in the absence (top panels) and in the presence (middle panels) of 8-Br-cAMP, were measured in records containing a maximum of two fully open channels. Data were distributed in bins of 100 ms. In all groups, $> 60\%$ of events were shorter than 2 seconds. The data show a trend towards increased frequency of short duration events for both wild-type and mutant channels following PKA activation. Black lines represent the best fits of the data. For Cx50 channels dwell open times were best fit with two time constants (untreated $R^2 = 0.84$: $\tau_1 = 1.03$ s, $\tau_2 = 3.9$ s; treated $R^2 = 0.80$: $\tau_1 = 0.83$ s, $\tau_2 = 3.7$ s), and those of the mutant with a single time constant (untreated $R^2 =$

0.64; $\tau=1.66$; treated $R^2=0.81$; $\tau=1.07$ s). The plots of differences (bottom panels) show, for Cx50, a small increase in events with durations < 500 ms (+11.4%) and a comparable decrease of all events with durations \geq 500 ms (-11.0%). For Cx50(S395A) events with durations < 500 ms increased (+4.6%) and those with durations \geq 500 ms decreased (-4.6%).

Fig. S5. The open time of specific open states in Cx50 junctions is minimally affected by PKA activation. Events were segregated by conductance to 0-89, 90-159 and >160 pS groups and their associated dwell open times plotted in 100 ms bins. Comparison of the untreated (left panels) and 8-Br-treated (right panels) Cx50 channels revealed only small increases (2.3, 2.3 and 6.5% for the 0-89, 90-159 and > 160 pS events, respectively) in the frequency of events with durations < 500 ms (with concomitant decreases in events \geq 500 ms duration).

Fig. S6. The open time of specific open states in Cx50(S395A) junctions is also minimally affected by PKA activation. Events were apportioned and plotted as in Fig. S4. Comparisons of the untreated (left panels) and 8-Br-treated (right panels) Cx50(S395A) channels revealed small increases (11, 4 and 5% for the 0-89, 90-159 and >160 pS events, respectively) in the frequency of events with durations < 500 ms.

Fig.S1

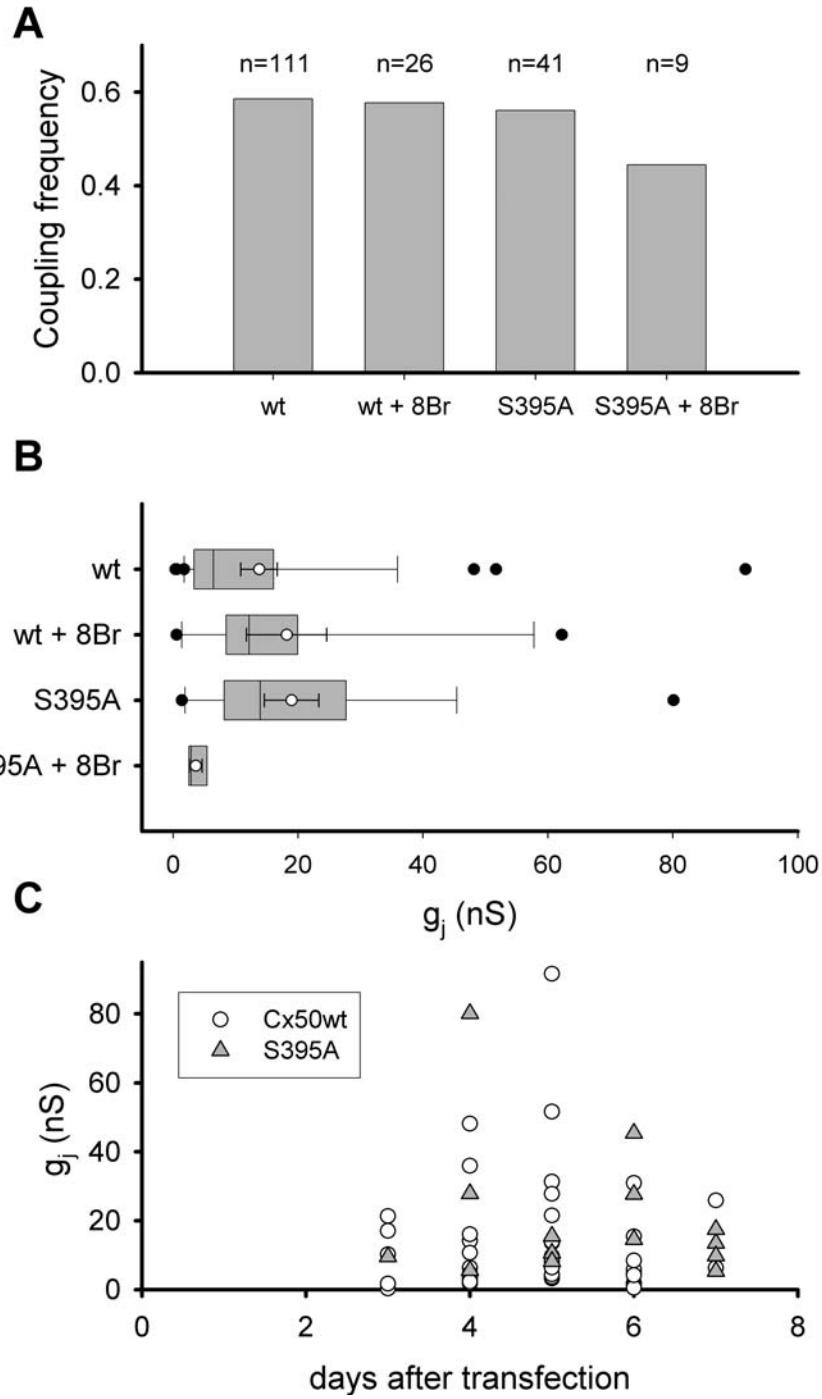


Fig.S2

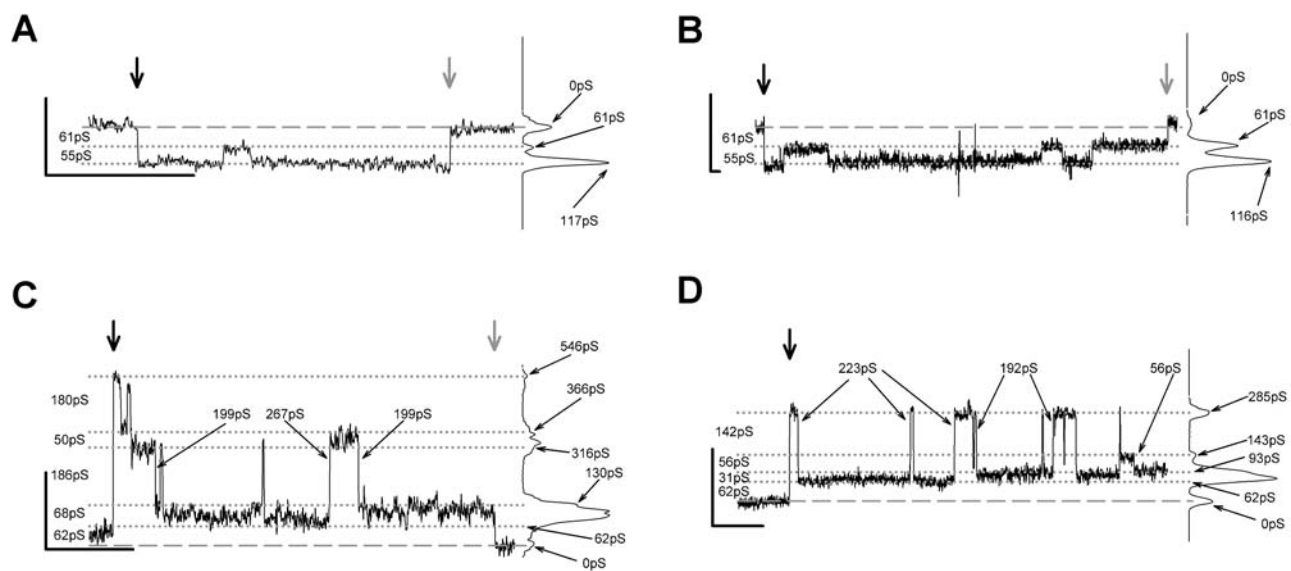
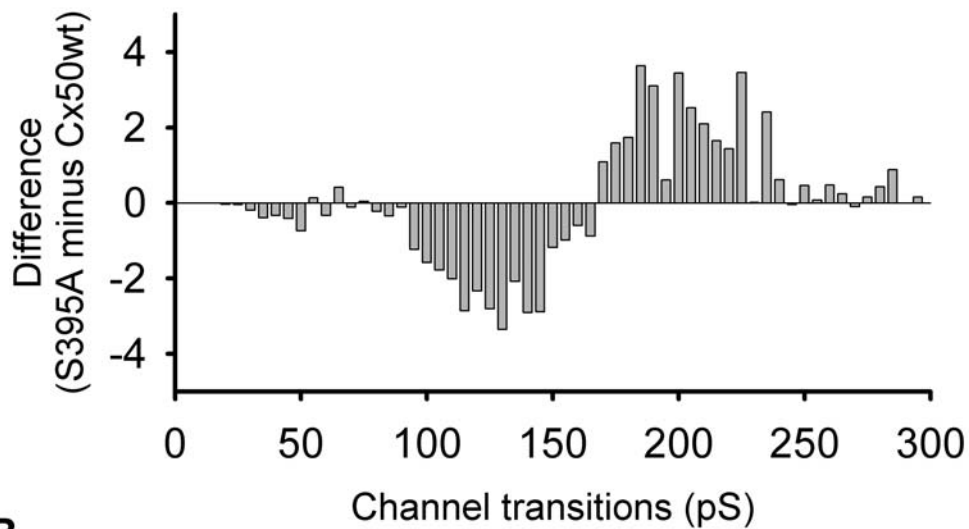


Fig. S3

A



B

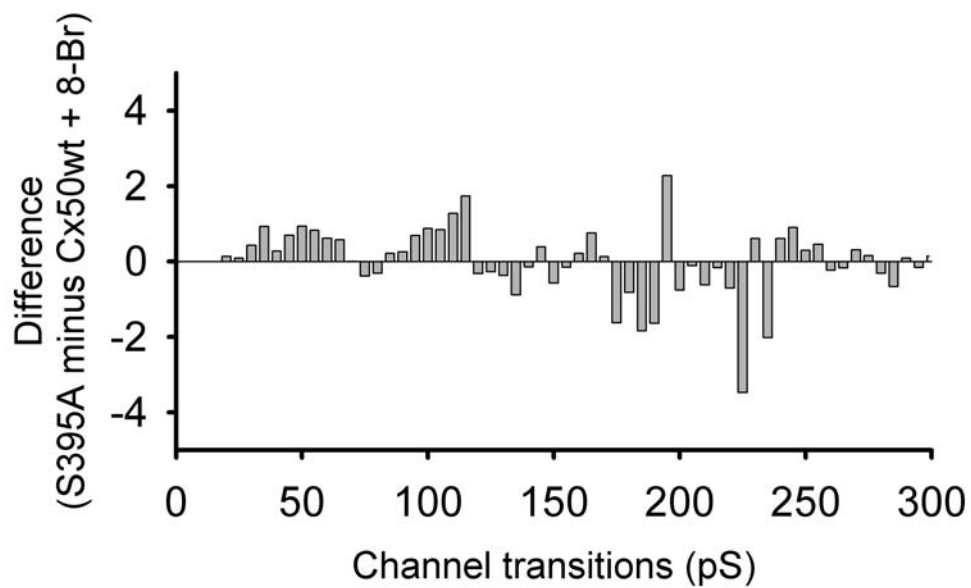


Fig. S4

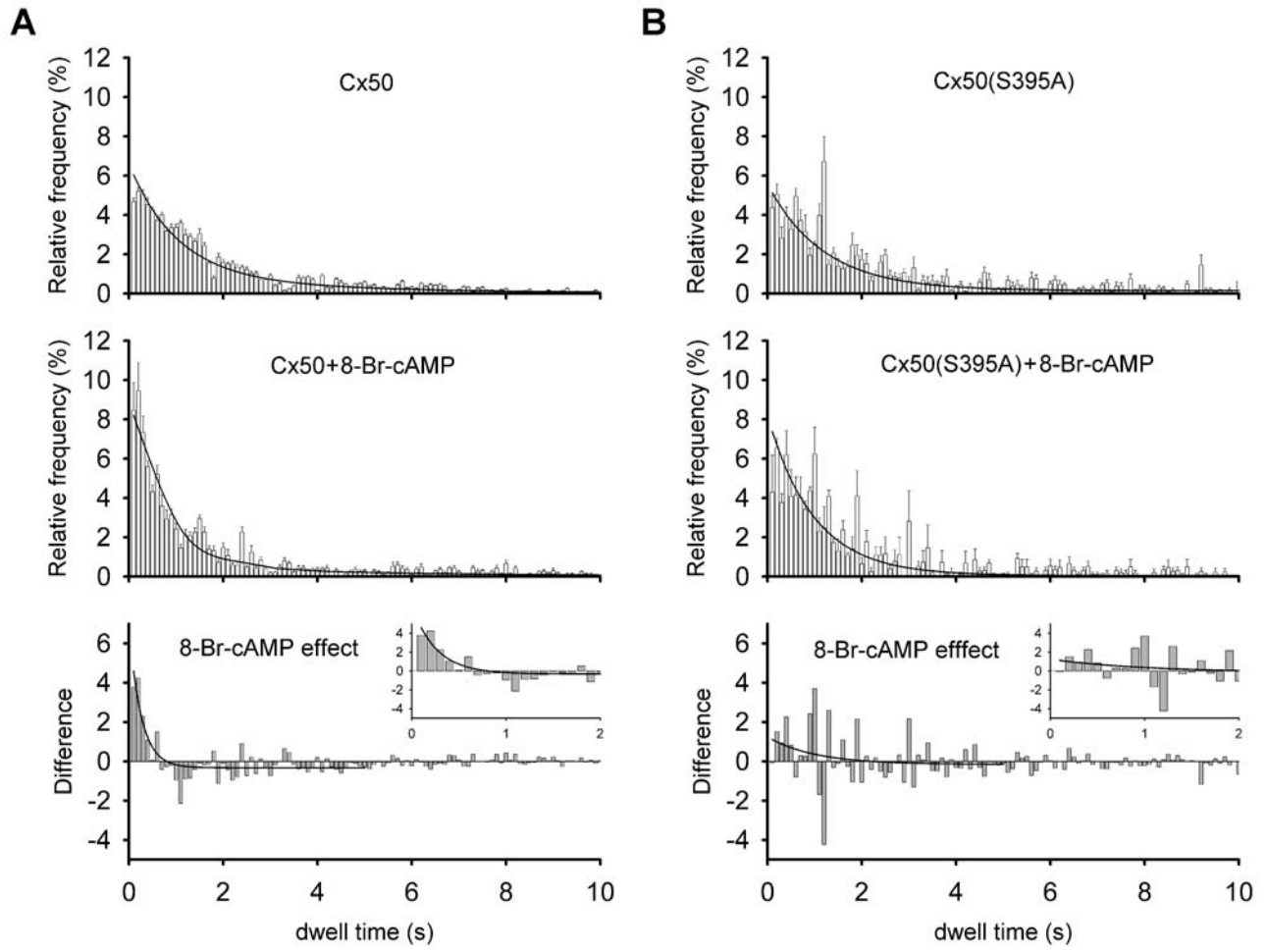


Fig. S5

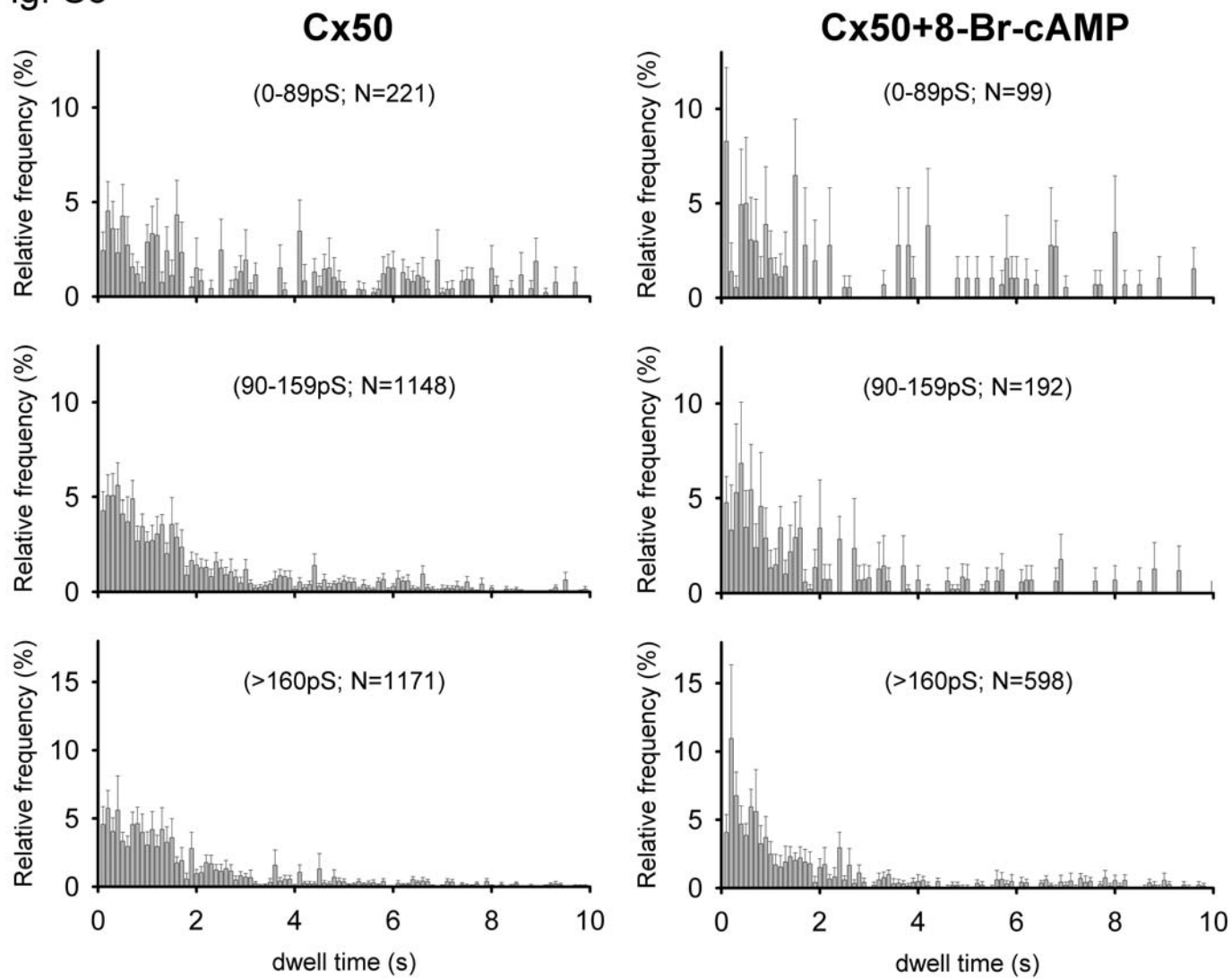


Fig.S6

